MAGNETIC RESONANCE IN CHEMISTRY, VOL. 36, 163–173 (1998)

A Nonlinear Regression Method for the Analysis of ^1H T_2 Dispersion Curves Including Comments on the Role of Polydispersity

M. A. K. Williams,* R. D. Keenan and T. K. Halstead

Department of Chemistry, University of York, Heslington, York YO1 5DD, UK

Received 26 May 1997; revised 2 October 1997; accepted 3 October 1997

ABSTRACT: A nonlinear regression method is described in detail for analysing ^1H T_2 (Carr–Purcell–Meiboom–Gill) dispersion curve measurements obtained from water-rich systems containing molecules possessing labile protons. The method is routine, provides well specified error statistics and does not make assumptions about the accessibility or mobility of the guest molecule site. The approach is validated using data simulated with the Carver–Richards two-site exchange model and experimental measurements carried out on a series of methanol-d_4–water mixtures of varying pH. Further simulations are described which investigate the role of polydispersity in determining the form of the dispersion curve and the relevance of the parameters extracted by fitting a composite curve to a single Carver–Richards function. The procedure is subsequently used to fit experimental dispersion curves originating from maltodextrin–water systems and the interpretation of the results is shown to be consistent with previously suggested ideas for molecular interactions in polysaccharide systems, involving discrete units of double helical nature, which can further aggregate to develop structure at a supramolecular level.

KEYWORDS: NMR; ^1H T_2 dispersion; proton exchange; biopolymer gels

INTRODUCTION

Largely as a result of the work of Hills and co-workers,[1–8] it is now generally recognized that proton exchange plays a major role in determining the transverse relaxation behaviour of water-rich systems containing molecules possessing labile protons. Systems of this type are common and range from relatively simple mixtures of liquids[4] to more complex biopolymer sols and gels,[1,2,6,7] which include those of particular interest to the food industry and the NMR imaging fraternity.[9]

Spin–spin relaxation times in the solution state are routinely measured using a Carr–Purcell–Meiboom–Gill (CPMG) pulse sequence,[10,11] which removes the effects of static field inhomogeneities by refocusing magnetization that has evolved under the influence of interactions that are linear in I_z. In practice, this means that the sequence is only effective for spins that are sufficiently mobile to yield negligible time-averaged quadrupolar and homonuclear dipolar interactions. The experiment consists of a train of equally spaced 180° pulses, which are applied to the sample to generate a sequence of spin-echoes. In the simplest case, the decay of the successive spin-echo heights is fitted to a single exponential function in order to extract a T_2 value. The sequence involves a user-defined delay time, 2τ, between the refocusing pulses which can routinely be varied between 10^{-4} and 10^{-2} s. Consequently, for systems in which the spins are undergoing chemical exchange at rates of the order of 1 kHz, such a variation of CPMG pulse spacing gives rise to a characteristic dispersion in the transverse relaxation behaviour.

A theoretical expression describing this variation of T_2 with τ has previously been developed in its most general form by Carver and Richards.[12] Hills *et al.*[3] have shown that experimental data from a number of real systems are amenable to analysis within the framework developed by Carver and Richards, and has also corrected a minor algebraic error in the original work. The model is cast in terms of five parameters, P_b, T_{2a}, T_{2b}, k and $\delta\omega$, where P_b is the fractional population of exchangeable protons on the guest molecule, T_{2a} and T_{2b} are the intrinsic spin–spin relaxation times of the respective sites (the subscript b denoting the guest molecule site and a the bulk water site), k is the exchange rate and $\delta\omega$ is the chemical shift difference between the sites.

Although the importance of proton exchange and the applicability of a corrected Carver–Richards expression to the analysis of T_2 data obtained from exchanging systems is now well recognized, reported studies to date have concentrated on methods of extracting selected physical parameters from the dispersion curve after initially estimating others. Typically T_{2a} has been estimated from the T_2 of neat water, T_{2b} from the relaxation time of non-exchangeable protons and P_b from the concentration of the guest molecule.[8] In the study of biopolymer systems, however, it is often not feasible to calculate P_b even if the concentration is known, owing to the possibility that molecular interactions may

* *Correspondence to*: M. A. K. Williams, Department of Chemistry, University of York, Heslington, York YO1 5DD, UK.
Contract grant sponsor: MAFF–DTI LINK.

 CCC 0749-1581/98/030163–11 $17.50

restrict the accessibility of some exchangeable protons. Although dispersion curves obtained from samples of the polysaccharide laminaran have been shown to be consistent with changes in P_b suggested from deuterium exchange studies,[5] there has not been a study of the feasibility of extracting the different physical parameters, including P_b and T_{2b}, from the direct fitting of experimental dispersion curves. Neither has there been an examination of the role of polydispersity in governing the apparent parameter values obtained from fitting composite data to a single Carver–Richards function. This paper seeks to address these points.

GENERAL FITTING PROCEDURE

Hills has stated that 'It is apparent that there are more unknown parameters than can be uniquely determined by simply fitting a dispersion curve.'[3,4,8] While indeed we found that it was not possible to extract all five Carver–Richards parameters by direct fitting, in a substantial number of cases simply knowing T_{2a} renders it possible to extract values of the other four quantities. Although T_{2a} may be slightly modified in the presence of guest molecules, it can be shown that if the value of T_{2a} is sufficiently long then the estimate of T_{2a} obtained by measuring T_2 in an independent experiment on a water sample containing no guest molecules is sufficiently accurate for our purpose. A fitting routine was written utilizing a non-linear regression based on the Levenberg–Marquardt algorithm[13] in which T_{2a} was user defined and T_{2b}, P_b, k and $\delta\omega$ were all free fitting parameters with user-defined starting values. The fitting was implemented within the environment provided by SPSS,[14] a widely available statistical package, which uses a modified Levenberg–Marquardt algorithm, proposed by Moré[15] and contained in MINPACK.[16]

Individual 95% confidence limits on each of the extracted parameters are also returned by the fitting procedure. These are appropriate for specifying confidence ranges in the individual parameters irrespective of the value of the other parameters.[17] It should be noted, however, that although separate confidence intervals of this type are often useful, caution must be exercised if attempts are made to interpret joint intervals. In cases where there is substantial covariance between parameters, it is possible that there may be a significant region of parameter space that, while giving acceptable joint solutions to 95% confidence, will not be included in the 95% confidence levels in the single parameter values. This does not change the definition of the 95% confidence in the single parameters, but affects how useful these values are in indicating a level of confidence region in higher dimensional parameter space. The fitting procedure also generates a correlation matrix which makes it possible to obtain an indication of the covariance between the different parameters. Although the non-linear regression methodology has recently been discussed in detail in an NMR context,[8] it has not previously been used in this manner to investigate the fitting of T_2 dispersion curves.

SIMULATIONS OF SINGLE DISPERSION CURVES

Sets of simulated dispersion curves were generated over an extensive range of parameter values. T_{2a}, P_b and $\delta\omega$ were fixed while nine values of both T_{2b} and k were used in all possible combinations, producing 81 dispersion curves. The sets of values were chosen to cover a range considered to be representative of a large number of systems of interest. The chosen k values started at 100 s^{-1} and subsequently spanned 250–2000 s^{-1} in 250 s^{-1} increments. The selected T_{2b} values were chosen between 1 and 10^{-4} s so that log T_{2b} values were equally spaced. The pulse spacings, τ, used in the simulations were spaced logarithmically in τ across the range from 10^{-4} to 10^{-2} s. Unless stated otherwise, T_2 values were generated for 10 pulse spacings per decade, giving a total of 21 points describing each simulated dispersion curve. Noise values were subsequently added to the simulated curves. These were obtained from a normal distribution of known standard deviation, typically 1–2% of $1/T_2$. These noise values are similar to those observed in practice, and this point is discussed again in due course.

Discussion of Fitting Results

For the purpose of obtaining a general impression of which regions of parameter space provided dispersion curves that, when fitted, gave 'reasonably accurate' estimates of the value of each parameter, the following criterion was adopted: if the ratio of an extracted parameter to the actual value used was between 0.95 and 1/0.95 then, in terms of the determination of the value of that parameter, the fit of that dataset was taken to be 'reasonably accurate.' The asymptotic 95% confidence limits returned by the fitting procedure were also examined. For the purpose of obtaining an impression of which combinations of parameters gave rise to fits in which the values of the extracted parameters obtained were 'reasonably precise,' the following criterion was adopted: if the difference between the 95% confidence limits and the extracted value of a particular parameter was less than 15% of the extracted value itself, then the fit was taken to be 'reasonably precise.' For sets of dispersion curves with fixed global values of T_{2a}, P_b and $\delta\omega$, the various values of $1/T_{2b}$ and k that gave 'reasonably accurate' or 'reasonably precise' results for each parameter were taken as coordinates and plotted in the $1/T_{2b}$–k plane, as shown in Fig. 1. Each symbol in the diagram represents a simulated dispersion curve, an open circle indicates that the value of the extracted parameter was 'reasonably accurate,' a cross that the value was 'reasonably precise' and only a small dot that the value was neither 'reasonably accurate' nor 'reasonably precise.'

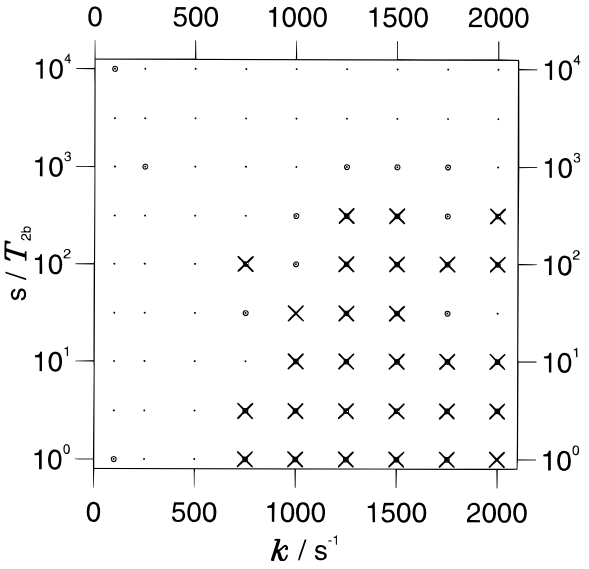

Figure 1. A plot summarizing the attempted extraction of P_b from the fitting of dispersion curves with 2% noise, $T_{2a} = 2.5$ s, $P_b = 0.005$ and $\delta\omega = 1885$ rad s^{-1}. 'Reasonably accurate' extraction of P_b (○), 'reasonably precise' extraction of P_b (×).

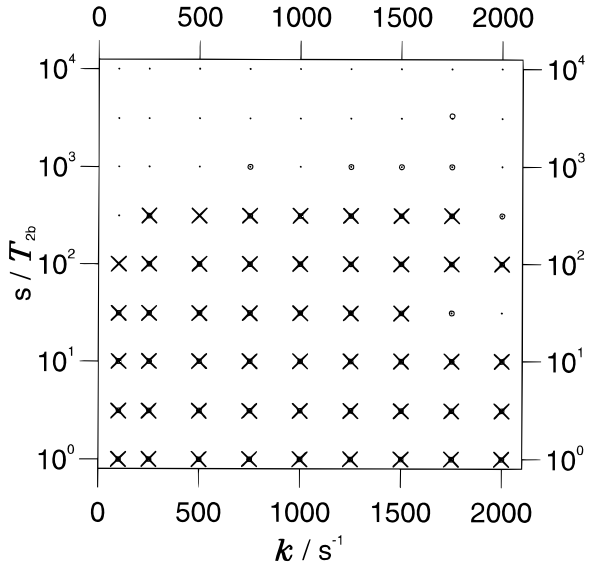

Figure 2. A plot summarizing the attempted extraction of $\delta\omega$ from the fitting of dispersion curves with 2% noise, $T_{2a} = 2.5$ s, $P_b = 0.005$ and $\delta\omega = 1885$ rad s^{-1}. 'Reasonably accurate' extraction of $\delta\omega$ (○), 'reasonably precise' extraction of $\delta\omega$ (×).

Owing to the criteria selected to define 'reasonably accurate' and 'reasonably precise,' minor changes in the fit resulting from different noise distributions were capable of causing the inclusion or exclusion of a point at particular parameter coordinates in subsequent runs of the simulation. However, user-defined variations of the values of the input parameters were found to produce dominant effects that were identifiable independent of the simulated noise distribution. In all fitting carried out in this work, the true values of each parameter were within the returned 95% confidence limits. There were no erroneous fits that gave incorrect parameter values to misleading precision. This demonstrates that regardless of the problems associated with the interpretation of uncertainties in a single parameter within a multi-parameter fit, the 95% confidence limits returned by the fitting procedure used here are useful.

Points in parameter space qualifying as 'reasonably precise' gave reasonable values of the corresponding extracted parameter, even if this value did not always fulfil the criterion set out here in order to be labelled as 'reasonably accurate.' The starting values of T_{2b}, P_b and k used in the fitting shown here were all twice the true values, while the initial estimates of $\delta\omega$ were set to be half of the true values used. The ratios of the starting estimates to the true values that still gave 'reasonably accurate' and 'reasonably precise' extractions depended significantly on the position of the dispersion curve in parameter space.

Figure 1 shows an example of a plot summarizing the fitting of dispersion curves generated with 2% noise, $T_{2a} = 2.5$ s, $P_b = 0.005$ and $\delta\omega = 1885$ rad s^{-1} (1 ppm at 300 MHz), with regard to the extraction of P_b. It should be noted that this value of P_b has been intentionally selected to be small, which is typical of many biopolymer systems of interest. Figure 2 shows the plot obtained for the extraction of $\delta\omega$. Similar plots were generated for k and T_{2b} but for brevity these are not shown.

It is apparent from the results of the analyses that both the accuracy and precision to which the different parameters can be extracted varies and is dependent upon the interrelation of the parameters and their relative importance in determining the form of the dispersion curve in different regimes. It should be noted that the correlation between the different parameters is also a function of their interrelation and relative value and that, in general, the parameters that are extracted well exhibit minor correlations. It is of general interest to determine whether or not it is possible to measure dispersion curves to sufficient accuracy to permit the extraction of useful values of any of the parameters, by regression analysis, from the direct fitting of the dispersion curves. This depends on the values of all parameters and indeed, in certain cases, it proved to be impossible to extract some of the parameters from simulations that incorporated experimentally realistic levels of noise. It is important to realize that the inability of the fitting procedure to extract one of the parameters does not necessarily preclude a fairly accurate and precise value being obtained for another, as can clearly be seen from a comparison of Figs 1 and 2. In fact, by performing a fit in this fashion a poorly estimated parameter with large 95% confidence limits may indicate that the dispersion curve does not depend significantly upon this property of the system and that its value is essentially unobtainable from this experiment.

By examining plots of the sort shown in Figs 1 and 2, generated for different global parameter sets and noise values, it is possible to draw some conclusions about the ability of the fitting procedure to determine the

Table 1. A selection of source dispersion curves which were used in combination to simulate the response of polydisperse systems

P_b	T_{2b} (s)	$\delta\omega$ (rad s^{-1})	k (s^{-1})	Set
0.001	1	1791	1750	1
0.001	0.1	2073	1375	2
0.001	0.01	1885	2500	3
0.001	0.001	1697	1000	4
0.001	0.0001	1979	2125	5
0.01	1	1697	2500	6
0.01	0.000 01	2073	1000	7
0.02	0.001	2073	1000	8
0.01	0.01	1791	2500	9
0.005	0.1	1979	1500	10
0.001	1	1697	2000	11
0.01	1	754	1000	12
0.000 778 7	0.000 04	628	1200	13

values of the different parameters. These observed trends can be rationalized by considering the evolution of the corresponding functional form of the dispersion curves. In general, if $1/T_{2b}$ or $k \gg \delta\omega$ the dispersive behaviour is drastically reduced and fitting the dispersion curve becomes impossible. Equally, if $1/T_{2b}$ or $k \ll \delta\omega$ then, although the dispersive effect may be large, there is little discrimination between the dispersion curves with different values of that parameter. The extraction of either T_{2b} or k is most effective when the value of that parameter is of the order of $\delta\omega$. As $\delta\omega$ increases the extraction of $\delta\omega$ and P_b becomes possible over a wider range of parameter sets and to an increasing degree of precision. At a 3% noise level the region of parameter space that provides dispersion curves, which, when fitted, still give good extractions of k and T_{2b} is reduced significantly compared with 2%. $\delta\omega$ and P_b are more robust but again the number of dispersion curves that give good extractions of these values is reduced markedly for noise levels greater than 2%.

SIMULATIONS OF DISPERSION CURVES FROM POLYDISPERSE SYSTEMS

Many systems of interest, such as biopolymer sols and gels, are likely, in reality, to be composed of a number of 'fractions' which may have significant variations in the values of the quantities that parameterize the Carver–Richards expression. Even in systems containing only carbohydrates where all labile protons are of the same chemical type, the chemical shift values may not all be identical. For example, in glucose solutions, at low temperature, the hydroxyl sites associated with the carbons at the 2-, 3- and 4-positions have been found to have chemical shift values which differ by 0.18 ppm.[18] A distribution of exchange rates is also possible and the T_{2b} values of distinct sites in polydisperse carbohydrate systems will, in general, depend on the length of the chain on which the site is situated.

In order to examine the implications of such polydispersity, sets of dispersion curves were generated in which T_{2b}, k and $\delta\omega$ were varied. A selection of these are summarized and labelled in Table 1. The curves were generated for a range of P_b values in order to simulate the response of polydisperse systems containing different amounts of the individual components. Assuming that there is no direct exchange of protons between guest molecule sites in different components the T_2 dispersion curve resulting from a polydisperse system can be generated by summing the individual dispersion curves due to the component fractions and then

Table 2. Results from non-linear regression fitting of composite set 1 + 2 + 3 + 4 + 5 (with $T_{2a} = 2.5$, av. $\delta\omega = 1885$ rad s^{-1}, av. $k = 1750$ s^{-1}, $P_b = 0.005$)

σ (%)	T_{2b} (ms)	P_b	$\delta\omega$ (rad s^{-1})	k (s^{-1})
1	1.84 ± 0.09	0.0064 ± 0.0009	1903 ± 196	1175 ± 407
	1.74 ± 0.08	0.0061 ± 0.0008	2018 ± 175	1215 ± 371
	1.79 ± 0.18	0.0056 ± 0.0004	1925 ± 265	1567 ± 338
2	1.68 ± 0.19	0.0061 ± 0.0015	2201 ± 236	1108 ± 510
	1.88 ± 0.27	0.0060 ± 0.0006	1818 ± 341	1446 ± 592
	1.78 ± 0.18	0.0063 ± 0.0016	2030 ± 467	1150 ± 607

Table 3. Results from non-linear regression fitting of composite set 6 + 7 (with $T_{2a} = 2.5$, av. $\delta\omega = 1885$ rad s^{-1}, av. $k = 1750$ s^{-1}, $P_b = 0.002$)

σ (%)	T_{2b} (ms)	P_b	$\delta\omega$ (rad s^{-1})	k (s^{-1})
1	1.38 ± 0.37	0.0193 ± 0.0017	1699 ± 362	1784 ± 720
	1.24 ± 0.12	0.0194 ± 0.0025	1922 ± 343	1430 ± 534
	1.23 ± 0.14	0.0187 ± 0.0025	1963 ± 411	1506 ± 670
2	1.28 ± 0.46	0.0180 ± 0.0017	1882 ± 670	1780 ± 1298
	1.24 ± 0.13	0.0209 ± 0.0072	2052 ± 468	1160 ± 841
	1.21 ± 0.11	0.0210 ± 0.0062	2085 ± 341	1140 ± 662

subtracting the extra water contributions. A large variety of composite dispersion curves were constructed in this manner, noise was added to the simulated data and the fitting procedure was carried out as described previously. The dispersion curves labelled 12 and 13 are taken from a previously proposed model of a hydrolysed starch system.[5]

Discussion of Fitting Results

The results of fitting the simulated dispersion curves originating from polydisperse systems to a single Carver–Richards function are shown for an illustrative number of examples in Tables 2–5. Each fit was performed a total of six times, each time using a different noise distribution with a standard deviation of 1 or 2%. In each case the weighted average of the constituent k and $\delta\omega$ values and the P_b value of the composite system are shown for comparison. It can be seen that, in general, the application of the fitting procedure described in this paper to dispersion curves resulting from polydisperse systems can still provide useful information. In the majority of cases the extracted k and $\delta\omega$ values are a useful indication of the average of those of the constituent components (weighted by the relative amount), while P_b is a clear indication of the total number of exchangeable protons, even in the case detailed in Table 3 where 50% of the simulated sample has a T_{2b} of 10 μs. The extracted value of T_{2b}, on the other hand, is much more difficult to interpret in these systems. This is perhaps due to the fact that the values associated with the individual 'fractions' can be spread over as many as five orders of magnitude, a substantially larger range than the other parameters. The results of the analysis on monodisperse systems carried out previously in this paper clearly show that not all T_{2b} values can be extracted with the same degree of accuracy and precision. Hence it appears that in polydisperse systems the extracted apparent value of T_{2b} depends not only on its constituent values but also on how successfully each of the constituent values can be extracted by the fitting procedure. The tendency here is to weight the apparent value of T_{2b} towards the millisecond range where $1/T_{2b}$ is of the order of $\delta\omega$.

EXPERIMENTAL VALIDATION

Having determined with the use of simulated data that the described fitting procedure provides a useful tool in the study of water-rich chemically exchanging systems, the approach was further validated by experiment. This involved both simple methanol–water mixtures and more complex maltodextrin–water systems.

The CPMG Experiment

Previous work has shown that careful CPMG experiments are capable of determining T_2 values to an accuracy and precision of 1–2%,[19] and it should immediately be noted that dispersion curves measured for such a dataset can often be usefully fitted, as demonstrated in the previous section. Other studies that have been concerned with the precision of T_2 measurements have concluded that the CPMG sequence is remarkably robust and that stability is the main requirement for a successful experiment.[20]

All NMR measurements were carried out using a Bruker MSL spectrometer operating at 300 MHz. The

Table 4. Results from non-linear regression fitting of composite set 8 + 9 + 10 + 11 (with $T_{2a} = 2.5$, av. $\delta\omega = 1971$ rad s^{-1}, av. $k = 1514$ s^{-1}, $P_b = 0.036$)

σ (%)	T_{2b} (ms)	P_b	$\delta\omega$ (rad s^{-1})	k (s^{-1})
1	2.09 ± 0.08	0.0312 ± 0.0013	1975 ± 131	1491 ± 272
	2.03 ± 0.06	0.0307 ± 0.0021	2147 ± 118	1370 ± 262
	2.22 ± 0.03	0.0307 ± 0.0020	1894 ± 114	1788 ± 445
2	2.14 ± 0.04	0.0357 ± 0.0090	2332 ± 183	949 ± 396
	2.33 ± 0.08	0.0319 ± 0.0070	1778 ± 338	1902 ± 815
	2.01 ± 0.16	0.0318 ± 0.0028	2070 ± 327	1477 ± 702

Table 5. Results from non-linear regression fitting of composite set 12 + 13 (with $T_{2a} = 3$, av. $\delta\omega = 741$ rad s^{-1}, av. $k = 973$ s^{-1}, $P_b = 0.010\,778\,7$)

σ (%)	T_{2b} (ms)	P_b	$\delta\omega$ (rad s^{-1})	k (s^{-1})
1	12.58 ± 1.45	0.0107 ± 0.0009	802 ± 68	832 ± 104
	16.67 ± 5.39	0.0134 ± 0.0038	677 ± 127	1018 ± 139
	15.73 ± 5.00	0.0130 ± 0.0036	695 ± 131	991 ± 151
2	15.20 ± 8.38	0.0126 ± 0.0060	707 ± 235	971 ± 281
	12.99 ± 3.84	0.0108 ± 0.0025	795 ± 160	892 ± 230
	13.55 ± 2.95	0.0114 ± 0.0020	767 ± 110	901 ± 151

temperature was set at 298 K unless stated otherwise and was controlled by a gas flow system, to within ± 1 K. The basic pulse sequence used was the standard CPMG sequence: 90°_x–(–τ–180°_y–τ–echo–)$_n$. Typical 90° pulse lengths were 12–13 μs using a 100 W amplifier. The experiments were carried out in external advance mode so that the ADC was only triggered at times corresponding to the spin-echo maxima. This ensured the most efficient sampling of the data and the direct acquisition of the decay curve. The recycle delay was set to $>5T_1$ to ensure fall magnetization recovery between applications of the pulse sequence. Eight scans of the decay curve were usually recorded, incorporating phase cycling, giving a typical signal-to-noise ratio of between 500 and 1000. The pulse programme was nested in a variable τ loop so that it was possible to measure a dispersion curve automatically. As this necessarily involved the sample being irradiated over substantial time periods, the effects of radiofrequency heating on the measured T_2 value were investigated and found to be negligible. In the automatic measurement of decay curves with variable τ the filter width was set according to the smallest τ delay. Sufficient echoes were obtained to give a stable baseline and particular attention was placed on observing that no baseline drift had occurred, which would be indicative of the presence of phase glitches or problems associated with diffusion in an inhomogeneous field,[21,22] and could lead to errors in the measurement of T_2.

Analysis of the Decay Curve

A non-linear regression based on the Levenberg–Marquardt[13] algorithm was used to fit the experimental decay curves to an exponential function. The correlation coefficient for such a fit is based upon the ratio of the sum of the squares of the residuals to the square of the spread of the values about their mean (which relates to the magnitude of the functional variation). While it is true that a small value of this ratio, often corresponding to a quoted correlation coefficient near unity, indicates that the residuals are small compared with the size of the functional variation, this is often misleading taken to imply that the chosen fitting function is a good representation of the data. In fact, this value is largely meaningless without a knowledge of the intrinsic noise present in the data. The value of the correlation coefficient does not convey any information about the relative contributions to the residuals of the actual intrinsic noise in the experimental data values and mismatches of the chosen fitting function. It is important in extracting T_2 values from fitting the CPMG decay curve not to use the correlation coefficient as the only criterion for judging the quality of the fit. Plotting the residuals is useful in this situation, as it immediately becomes apparent whether the residuals are randomly scattered, which would be expected if the chosen functional form is a good fit to the data, or show a systematic variation. However, this procedure is somewhat subjective. A better approach is to calculate reduced chi-squared, χ_s^2, defined as the ratio of the mean square residuals obtained from the fit (s^2) to the mean square of the intrinsic noise in the data (σ^2). For a perfect fit the only residuals result from the intrinsic noise and $\chi_s^2 = 1$. This type of analysis has been discussed previously, in detail, in relation to multi-exponential fitting.[23] In this work, σ^2 was calculated for each decay curve from the baseline and s^2 for each fit was returned by the fitting procedure. In this manner, estimated χ_s^2 values were recorded for the fitting of each decay curve as a further check on the extracted values of T_2. As both the fit itself and the intrinsic noise value calculation were carried out on a limited number of points, some variation of χ_s^2 from 1 is to be expected. It was assumed that χ_s^2 values as large as 1.5 were acceptable fits[24] under typical experimental circumstances, and all fits reported here fulfilled this criterion.

Methanol–water

Sample Preparation. Methanol-d_4–water mixtures were prepared and the pH values of the solutions were varied by the addition of NaOH and HCl. The composition was chosen so that $P_b = 0.0419$, in line with a previous study.[4] Since methanol-d_4 was used, *ca.* 4% of the total exchangeable proton sites were occupied by deuterons. This was preferable to using protonated methanol where the signal from the non-exchangeable methyl protons would have necessitated double exponential fitting of the magnetization decay. The pH reported here was measured with a glass electrode after sample preparation was completed.

Results and Discussion. Figure 3 shows typical dispersion curves obtained from a study carried out on methanol-d_4–water mixtures of varying pH and fits

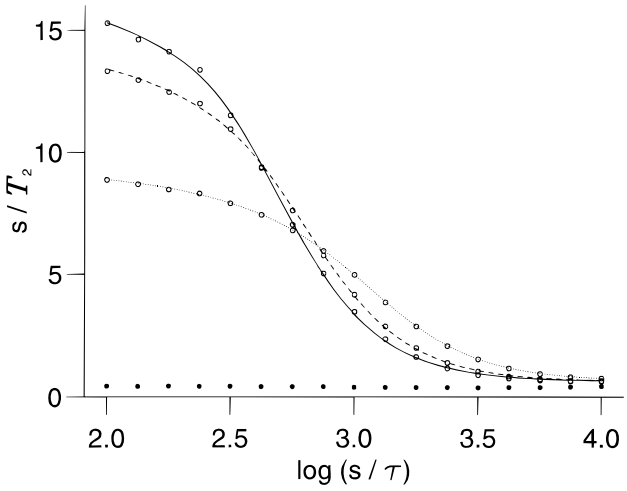

Figure 3. Dispersion curves obtained from a study carried out on methanol-d_4–water mixtures (○) of pH 7.0 (—), 7.5 (– –) and 8.2 (· · ·), with fits obtained from the application of a non-linear regression analysis described in this work. The results obtained from the neat water used are also shown (●).

obtained from the application of a non-linear regression analysis described in this work. The results obtained from a neat water sample are also shown and can be seen to have negligible variation. (A simplistic calculation of the contribution to dispersive behaviour resulting from the exchange of protons between sites on water molecules adjacent to ^{17}O and ^{16}O nuclei, respectively, concurs with this observation for naturally occurring isotopic abundances.) It can be seen that there is excellent agreement between the experimental and fitted curves. The values of the Carver–Richards parameters extracted by the fit are shown in Table 6, in comparison with values obtained in previous work at similar pHs.[4] The quoted uncertainty values are 95% confidence limits.

Figure 4 shows the exchange rates obtained from both studies plotted as a function of pH. Two theoretical predictions, taken from the work of Hills,[4] are also shown (i) for a purely acid–base-catalysed exchange mechanism and (ii) for an exchange process which includes a contribution from a neutral mechanism. It can be seen that there is good agreement between the experimental results, and in particular that the value of the exchange rate at neutral pH is significantly greater than that predicted by a purely acid–base-catalysed mechanism. This provides further evidence that neutral exchange mechanisms exist in this system. This has been discussed in detail by Hills[4] and is not the focus of this paper, although it should be noted that having 95% confidence limits for the extracted exchange rate values strengthens the case against a purely acid–base-catalysed mechanism.

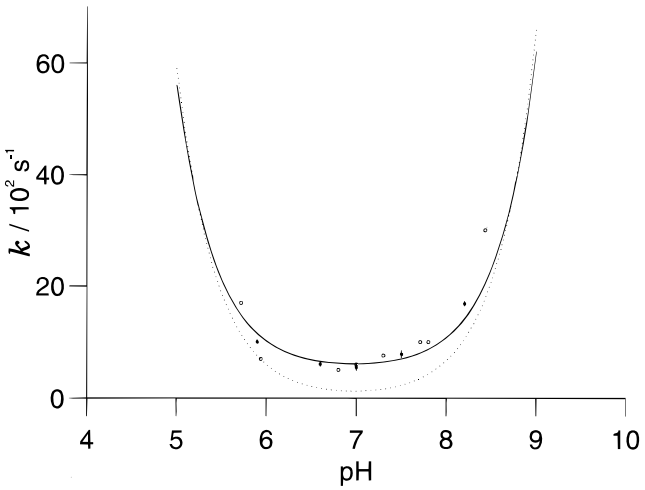

Figure 4. The exchange rates obtained from both this work (●) with 95% confidence limits and Ref. 4 (○), plotted as a function of pH. Theoretical predictions, taken from Ref. 4, are also shown (i) for a purely acid–base catalysed exchange mechanism (···) and (ii) for an exchange process which includes a contribution from a neutral exchange mechanism (—).

While the values of the parameters obtained from the different studies cannot be compared directly with one another because the measurements were made at slightly different pHs (with the exception of pH 7.0), Table 6 is still of general interest. The $\delta\omega$ values obtained by both studies give similar chemical shift values, and those obtained in this work are the same within experimental uncertainty. Chemical shift differences exhibited by the hydroxyl protons of methanol compared with those of water have previously been measured in alcohol–water mixtures by using deuterated solvents and low temperatures.[25] Taking account of the differences in the temperature coefficient of chemical shift between the two sites, a $\delta\omega$ value of *ca.* 0.31 ppm at 298 K can be predicted. This is in good agreement with the values reported here and this gives further confidence in the fitting procedure.

The intrinsic relaxation rates of the hydroxyl protons reported in this study are all, as found previously,[4] considerably faster than obtained for pure methanol (measured in an independent experiment to be 0.312 s^{-1}) and are, within 95% confidence limits, independent of pH, having a mean value of the order of 4 s^{-1}. The contribution to the transverse relaxation rate of a methanol hydroxyl proton in dilute aqueous solution from the fluctuation of intermolecular proton–proton interactions, resulting from the diffusion of water molecules, is of the order of 0.1 s^{-1}. It seems reasonable, therefore,

Table 6. Carver–Richards parameters obtained from the application of the fitting procedure to experimental dispersion curves obtained from methanol-d_4–water mixtures of varying pH (a) in comparison with values obtained at similar pH values in previous work (b)[4]

pH	k (s^{-1})	$\delta\omega$ (ppm)	T_{2b} (s)	P_b	Source
5.9	1006 ± 34	0.29 ± 0.04	0.35 ± 0.17	0.065 ± 0.041	(a)
5.94	700	0.310	0.23	—	(b)
6.6	606 ± 37	0.29 ± 0.02	0.24 ± 0.07	0.055 ± 0.021	(a)
6.80	500	0.312	0.35	—	(b)
7.0	548 ± 55	0.29 ± 0.02	0.23 ± 0.09	0.058 ± 0.021	(a)
7.00	600	0.324	0.62	—	(b)
7.5	784 ± 66	0.32 ± 0.03	0.19 ± 0.08	0.048 ± 0.010	(a)
7.30	760	0.337	0.63	—	(b)
7.71	1000	0.318	0.35	—	(b)
8.2	1684 ± 41	0.33 ± 0.05	0.17 ± 0.09	0.047 ± 0.020	(a)
8.43	3000	0.341	0.84	—	(b)

to suggest that the increase in the relaxation rate is due to a lengthening of the reorientational correlation time of the methanol molecule in the mixtures, by as much as an order of magnitude, compared with that in the neat liquid. There is some evidence to support this: the diffusion coefficient for methanol in water is found to be 70% of the methanol self-diffusion coefficient, and it has previously been suggested from chemical shift measurements[26] that methanol is less strongly hydrogen bonded in methanol than in water.

The values of P_b extracted by the fitting procedure are all the same within 95% confidence limits, as expected, and for each curve the true value is within the calculated uncertainty. In these experiments P_b was known and could have been fixed initially. However, for an arbitrary system this is not always the case and it is the purpose of this work to demonstrate the general applicability of the described fitting procedure.

Maltodextrin–water

Sample Preparation. Maltodextrin was obtained from Cerestar UK. The sample was an α-amylase degraded potato starch that was initially *ca.* 60% amylopectin. Samples of various concentrations were prepared by adding a known weight of maltodextrin to a known weight of deionized water. These mixtures were then heated for 30 min in a water-bath maintained at 358 K while the solutions were continuously stirred. Samples were contained in flasks sealed with Parafilm, to reduce evaporation, and were weighed after preparation. Some of the sample was then transferred, using a glass pipette, into an NMR tube (5 mm o.d.). The glassware was kept warm in an oven to prevent the sample experiencing large thermal gradients at this stage. The samples were subsequently left to cool to room temperature. The pH of each sample was measured and found, at pre-gelling temperatures, to be *ca.* 5.7 ± 0.2. An independent measurement of the proton NMR relaxation time, T_2, of the neat water used to prepare the samples was also performed. Repeat experiments carried out on a replicate 1% (w/w) sample were found to produce consistent decay curves and T_2 values in agreement to better than 1%. With biopolymer gels, assessing the repeatability of T_2 measurements is complicated by the difficulty of reproducing samples of exactly the same concentration that have had identical thermal histories. Deviations in this respect could possibly yield states of the system that differ at the molecular level. However, 24 h after the gels had cooled, any changes in these systems were believed to be occurring relatively slowly, so that T_2 experiments repeated many times over the time-scale of minutes were assumed to be on an identical system.

The Gelation of Amylose and Amylopectin. The gelling behaviour of a maltodextrin solution will be dependent upon the relative proportions of (linear) amylose and (branched) amylopectin it contains. It is worthwhile, therefore, to review briefly the behaviour of amylose and amylopectin solutions.

Early studies of amylose gelation observed that above 1.5% (w/w) amylose forms a gel rather than a precipitate.[27] It was concluded from viscosity data that this critical gelling concentration corresponded to the coil-overlap concentration. In 1989, however, a series of papers were published on the aggregation and gelation of nearly monodisperse enzymically synthesized amylose fractions, which showed that, for amyloses with a degree of polymerization (DP) >250, gels formed at $>1\%$ (w/v) concentration, independent of chain length and, in contrast to the previous work, below the coil-overlap concentration.[28–30] A more recent study, carried out on an amylose sample obtained from a potato starch fraction, found a value for the overlap concentration of twice that reported previously for the same DP, further distancing this value from that of the critical gelling concentration.[31] The value of the overlap concentration obtained in that study was justified by calculating a critical molecular weight for the onset of entanglements and relating it to certain structural parameters of amylose.

The non-equivalence of the critical gelling concentration and the coil-overlap concentration has previously been observed for globular proteins[32,33] and suggests that a specific cross-linking mechanism is responsible for the gelation behaviour. The molecular units that result from such cross-linking in amylose have been shown, by ^{13}C cross-polarization magic angle spinning (CP/MAS) NMR, to be composed of double helices of the B-type.[30] In this model, the formation of molecular units is the initial process that underlies gelation and the subsequent development of long-range order results from the packing of the double helical units. Similarly, it has been suggested from studies of the disruption of starch granules, that the integrity of the granules largely results from interactions at the double helical level.[34] The results of a Fourier transform IR study concur with the notion that coil to helix transitions are at the heart of both amylose and amylopectin gelation, being intermolecular and intramolecular, respectively.[35]

An early study of the gelation of amylopectin found that although the coil-overlap concentration, deduced from viscosity data, was 0.9% (w/w), gelation only occurred from 'heavily entangled' solutions of $>10\%$ concentration.[36] This behaviour is distinctly different from that of amylose, where gels are known to form well below the coil-overlap concentration. This is not entirely unexpected, however, considering that linear chain sections of the length thought to be involved in the intermolecular interactions of amylose (*ca.* 100 residues) are not present in the branched amylopectin structure. A later study,[37] in which an even greater critical gelling concentration of 18% was found, suggested that the critical concentration depended on molar mass. More recently it has been shown that weak amylopectin gels can be formed at lower concentrations (3%), which are visually clear and homogeneous.[38] It has been proposed that the mechanism of gelation in this case is the

pairwise aggregation of outer amylopectin chains to form double helices.

Results and Discussion. Typical CPMG decay curves, obtained from samples 24 h after preparation, were found to be good fits to single exponential functions (based on the criteria discussed in the Experimental section). It is assumed that the signal from non-exchangeable biopolymer protons was either small enough to be negligible or, at the higher concentrations, short enough to have dephased before the observation of the first echo. In a previous NMR study that used CPMG measurements of ^{1}H T_2 to investigate the structure of systems containing amylose, amylopectin and their mixtures,[39] single exponential decay curves were reported for concentrations of maltodextrin up to 12%. Unfortunately, the CPMG pulse spacing was not specified and, furthermore, chemical exchange between the bulk water and the biopolymer hydroxyl groups was completely ignored, casting serious doubt on the interpretation presented.

Figure 5 shows the results of typical ^{1}H T_2 dispersion experiments carried out on maltodextrin samples of biopolymer weight fraction 1, 5, 10, 15 and 20% (w/w) (uncorrected for moisture content). The solid lines are fits to the data with $T_{2a} = 2.48$ s in all cases (this value was chosen to be equal to the independently measured value of the T_2 of the bulk water used in the preparation of this set of samples). The fits were obtained as described previously. It can be seen that there is excellent agreement between the experimental data and the fitted functional forms. The extracted values of k and $\delta\omega$ varied slightly, but not significantly within 95% confidence limits, as a function of concentration. The averages of these extracted values (weighted by the reciprocal of the variances of each fit) were 901 ± 46 Hz and 1.00 ± 0.05 ppm, respectively. It is clear from the results obtained using simulated systems that for a system of this type these should be interpreted as indicating the average values of any distinct sites. It is interesting to note that the average of the chemical shift values obtained from the hydroxyl protons at the 2-, 3- and 6-positions for α-D-glucose at 273 K is 1.00 ppm.[18] The extracted T_{2b} values varied from 10 ms in the most dilute sample to *ca.* 4 ms for the more concentrated systems. However, these results should be treated with caution owing to the significant polydispersity of the sample. This is discussed again in due course.

Figure 6 shows the variation in the value of P_b, extracted by the fitting procedure for a set of maltodextrin sols and gels, as a function of the percentage biopolymer weight fraction, w. These weight fractions were calculated taking into account the moisture content of the maltodextrin sample. It is interesting to consider the expected form of a plot of P_b *vs.* w based on simplistic models for the behaviour of maltodextrin–water systems.

In general, in the absence of any conformational change or specific interactions that would restrict the accessibility of some exchangeable groups on the biopolymer, P_b would be expected to be of the form

$$P_b = \left[1 + \left(\frac{M}{9n}\right)\left(\frac{100 - w}{w}\right)\right]^{-1} \quad (1)$$

where M is the relative molar mass of a biopolymer residue and n is the number of exchangeable protons per residue. In the case of maltodextrin, $M = 162$ and n can be estimated from the structures of amylose and amylopectin as follows. Each of the glucose monomers that constitute the amylose backbone has three hydroxyl protons that are potentially exchangeable. This is also true of the branched amylopectin structure, with the exception of the glucose unit that forms the branching point at the 6-position. It is believed that

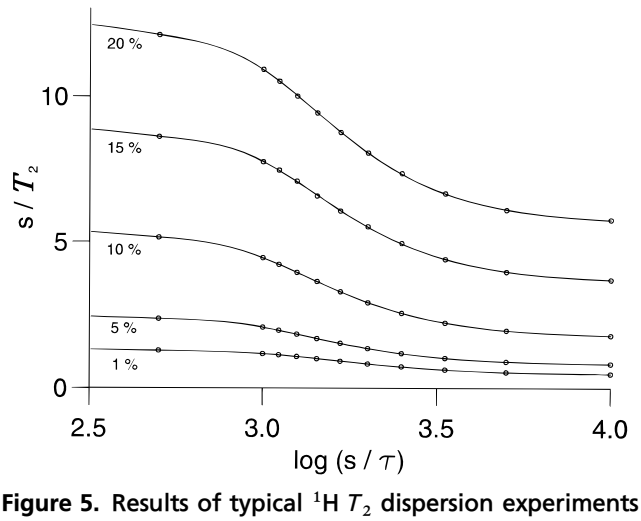

Figure 5. Results of typical ^{1}H T_2 dispersion experiments (○) carried out on maltodextrin samples of biopolymer weight fraction 1, 5, 10, 15 and 20% (uncorrected for moisture content). The solid lines are fits to the data carried out as described in the text.

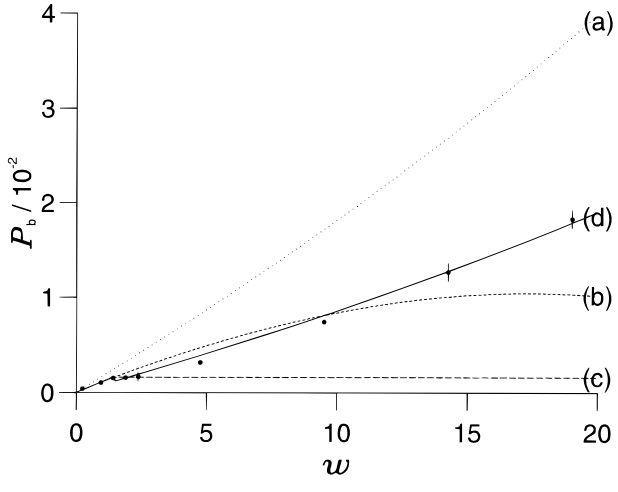

Figure 6. The variation in the value of P_b (●), extracted by the fitting procedure, with 95% confidence limits, for a set of maltodextrin sols and gels, as a function of w. These weight fractions were calculated taking into account the moisture content of the maltodextrin samples. The curves are generated model functions described in the text.

typically there is a branching point every 20–25 units[36] in the amylopectin structure so that, on average, amylopectin has 2.95 exchangeable protons per residue. In the production of maltodextrin, because the enzymatic cleavage of glycosidic bonds in starch proceeds via hydrolysis, further exchangeable hydroxyl sites are introduced, the number of which will depend on the resulting molar mass distribution. It is not unreasonable, in a simplistic model, to assume a value of three exchangeable protons per residue for the maltodextrin and the functional form given by Eqn (1) is plotted in Fig. 6 [curve (a)], based on this value. It is immediately apparent that this function significantly overestimates the number of exchangeable protons available compared with the value obtained from the fitting of the experimental dispersion curves. The work on the simulated dispersion curves clearly shows that this large discrepancy in this measured exchangeable fraction is not an artifact of polydispersity. Neither can changes in T_{2a} resulting from the motion of constrained water molecules provide an explanation. Fitting data which originate from a system with low T_{2a} to a Carver–Richards function with T_{2a} erroneously set to a higher value can only yield a P_b value that is higher than the true value. Clearly, the discrepancy between the experimentally determined P_b values and those calculated assuming all exchangeable protons contribute to fast chemical exchange warrants a physical interpretation.

For data obtained up to and including $w = 1.5\%$, a fit to Eqn (1) yields $n = 2.1 \pm 0.3$. This suggests that even in the low concentration region a fraction $f_1 \approx 1/3$ of the hydroxyl protons are not contributing to the dispersive behaviour. It has recently been proposed that intramolecular hydrogen bonding occurs between the OH(6) and the adjacent hemiacetal oxygen atom of the D-glycosyl residues of amylose molecules in aqueous solution.[40] This would be consistent with our observations if it were postulated that protons involved in intramolecular hydrogen bonds were removed from the pool taking part in fast chemical exchange.

In order to explain the observed variation of P_b above 1.5%, however, it was found necessary to take into account both intra- and intermolecular interactions. In this context, the distinct models in which hydroxyl protons are prevented from participating in fast chemical exchange were considered.

Model 1

In the case of progressive entanglement, as the concentration rises an additional fraction of exchangeable protons ($f_2 w$) would become inaccessible as the biopolymer becomes increasingly entangled. It has been assumed here that the number of interaction points is proportional to w, although it is possible that the dependence is on w^n with $n > 1$ (it should be remembered that the r.m.s. end-to-end distance of a random coil is proportional to $(DP)^{1/2}$, so that the probability of entanglement will depend not only on the total mass of the biopolymer present but also on the polydispersity of the sample). In this case, the dependence of n on w is given by

$$n = 3(1 - f_1 - f_2 w) \tag{2}$$

where f_1 and $f_2 w$ are the fractions per residue of exchangeable biopolymer protons removed from fast chemical exchange by intramolecular and intermolecular interactions, respectively. Curve (b) in Fig. 6 was calculated using Eqns (1) and (2) with $f_1 = 1/3$ and f_2 set to give good agreement with experiment in the centre of the examined concentration range.

Model 2

In the opposite extreme, a 'crystallization' process can be envisaged in which the further addition of maltodextrin to an aggregated system would simply increase the dimensions of the aggregate. In this case the number of the extra exchangeables provided by the addition of new material would be equal to those removed at the interaction site. The predicted functional form resulting from this scenario would be given for $w < 1.5$ by Eqns (1) and (2) with $f_1 = 1/3$ and $f_2 = 0$ and for $w > 1.5$ by $P_b = P_b(1.5)$, as shown in Fig. 6 [curve (c)].

Model 3

Maltodextrin solutions above a critical concentration could be involved in intermolecular pairwise aggregation, forming double helices. This would result in a further fraction of protons per residue, f_3, becoming inaccessible, in addition to those involved in intramolecular interactions, so that the predicted functional form resulting from this process would be given for $w < 1.5$ by Eqns (1) and (2) with $f_1 = 1/3$ and $f_2 = 0$ and for $w > 1.5$ by Eqns (1) and (3):

$$n = 3(1 - f_1 - f_3) \tag{3}$$

The case of $f_1 = 1/3$ and $f_3 = 1/5$ is shown in Fig. 6 [curve (d)]. It can be seen that this is by far the most successful description of the experimental data. This is also in fair agreement with a proposed model of intermolecular hydrogen bonding for amylose in aqueous solution, in which pairwise associations of the molecules are stabilized by hydrogen bonding between the OH(2) and adjacent O(6) of the D-glucosyl residues on different molecules,[40] as in the solid state. This process would be expected to involve one extra hydroxyl site per two residues compared with the intramolecular situation, which would be equivalent to $f_3 = 1/6$. The slight discrepancy between this theoretical value and that determined experimentally could possibly be the result of the further aggregation of double helical regions, involving specific interhelical interactions.

In conclusion, the experimental data shown in Fig. 6 suggest the formation of discrete molecular units, which

is consistent with the model of double helix formation suggested by Gidley.[30]

It would be expected that the formation of double helical structures would also be reflected in the molecular dynamics of the biopolymer and hence in T_{2b}. However, it is not straightforward to predict the exact form of the relationship between T_{2b} and concentration. T_{2b} is inversely proportional to the residual magnetic dipole–dipole interaction experienced by the proton and although, qualitatively, the more rigid a gel becomes the larger the residual static interaction and the shorter T_{2b} becomes, the exact form of the averaging behaviour is complex. Even if this function could be elucidated, the present work on the simulated polydisperse systems indicates that the T_{2b} values extracted depend in a complicated way on the efficiency of the fitting routine in different T_{2b} regimes and, although T_{2b} values of the order of milliseconds are reasonable, this does not preclude the existence of many other dynamic environments.

CONCLUSIONS

It has been shown, both with the use of simulated data and experimentally, that a four-parameter non-linear regression analysis of ^{1}H T_2 dispersion curves can be a useful tool in the study of water-rich systems, in which spins are undergoing proton exchange, even if the size of the exchangeable population is unknown and significant polydispersity exists. The application of the fitting procedure is routine and has the advantage of producing well defined 95% confidence limits. The work carried out with simulated data provides an understanding of the ability of the fitting procedure to extract accurate and precise values of the physical quantities parametrizing the Carver–Richards expression. This is of general interest and provides not only an interpretation of fitting results but also a basis for experimental design, where the optimum values of external parameters such as applied field strength, temperature and pH could be chosen to give the best chance of the successful extraction of a particular parameter.

It has also been shown that the procedure is successful in fitting experimental dispersion curves obtained from maltodextrin–water systems. The extracted P_b values are found to be considerably lower than those calculated on the basis of the maltodextrin structure assuming that all hydroxyl protons contribute to fast chemical exchange. Extensive simulations of polydisperse systems have shown that this observed reduction cannot be accounted for by the effects of sample polydispersity. The simplest interpretation of the results is consistent with previously postulated mechanisms of molecular interaction: at low concentration ($<1.5\%$ in this work) one hydroxyl group per residue is involved in intramolecular hydrogen bonding and is therefore not involved in fast chemical exchange processes. At higher concentrations, discrete units of double helical nature are formed which are stabilized by intermolecular hydrogen bonding. These molecular units can further aggregate to develop structure at a supramolecular level.

Acknowledgements

This work was supported by a MAFF–DTI LINK programme, 'The Behaviour of Biopolymer Mixtures in Structuring Food Products.'

REFERENCES

1. B. P. Hills, S. F. Takacs and P. S. Belton, *Mol. Phys.* **67**, 903 (1989).
2. B. P. Hills, S. F. Takacs and P. S. Belton, *Mol. Phys.* **67**, 919 (1989).
3. B. P. Hills, K. M. Wright and P. S. Belton, *Mol. Phys.* **67**, 1309 (1989).
4. B. P. Hills, *J. Chem. Soc., Faraday Trans.* **86**, 481 (1990).
5. B. P. Hills, C. Cano and P. S. Belton, *Macromolecules* **24**, 2944 (1991).
6. B. P. Hills, *Mol. Phys.* **76**, 489 (1992).
7. B. P. Hills, *Mol. Phys.* **76**, 509 (1992).
8. B. P. Hills, *Signal Treatment and Signal Analysis in NMR*. Elsevier, Amsterdam (1996).
9. E. Liepinsh and G. Otting, *Magn. Reson. Med.* **35**, 30 (1996).
10. H. Y. Carr and E. M. Purcell, *Phys. Rev.* **94**, 630 (1954).
11. S. Meiboom and D. Gill, *Rev. Sci. Instrum.* **29**, 688 (1958).
12. J. P. Carver and R. E. Richards, *J. Magn. Reson.* **6**, 89 (1972).
13. D. W. Marquardt, *J. Soc. Ind. App. Math.* **11**, 431 (1963).
14. *SPSS for Windows Advanced Statistics Release 6.1 Manual*, SPSS, SK 46 SPS/S (1994).
15. J. J. Moré, *Lecture Notes in Math*, No. 630. Springer, Berlin (1977).
16. Minpack, *Argonne National Labs Report*, ANL-80-74.
17. N. R. Draper and H. Smith, *Applied Regression Analysis*. Wiley, New York (1981).
18. J. M. Harvey, M. C. R. Symons and R. J. Naftalin, *Nature (London)* **261**, 435 (1976).
19. R. L. Vold, R. R. Vold and H. E. Simon, *J. Magn. Reson.* **11**, 283 (1973).
20. U. Haeberlen, H. W. Spiess and D. Schweitzer, *J. Magn. Reson.* **6**, 39 (1972).
21. D. G. Hughes and G. Lindblom, *J. Magn. Reson.* **26**, 469 (1977).
22. D. G. Hughes and G. Lindblom, *J. Magn. Reson.* **26**, 481 (1977).
23. N. J. Clayden and B. D. Hesler, *J. Magn. Reson.* **98**, 271 (1992).
24. P. R. Bevington and D. K. Robinson, *Data Reduction and Error Analysis for the Physical Sciences*. McGraw-Hill, New York (1992).
25. J. M. Harvey, S. E. Jackson and M. C. R. Symons, *Chem. Phys. Lett.* **47**, 440 (1977).
26. B. Kingston and M. C. R. Symons, *J. Chem. Soc., Faraday Trans. 2* **69**, 978 (1973).
27. H. S. Ellis and S. G. Ring, *Carbohydr. Polym.* **5**, 201 (1985).
28. M. J. Gidley and P. V. Bulpin, *Macromolecules* **22**, 341 (1989).
29. A. H. Clark, M. J. Gidley, R. K. Richardson and S. B. Ross-Murphy, *Macromolecules* **22**, 346 (1989).
30. M. J. Gidley, *Macromolecules* **22**, 351 (1989).
31. B. Jauregui, M. E. Muñoz and A. Santamaria, *Polymer* **34**, 1776 (1993).
32. A. H. Clark and S. B. Ross-Murphy, *Adv. Polym. Sci.* **83**, 57 (1987).
33. A. H. Clark and S. B. Ross-Murphy, *Br. Polym. J.* **17**, 164 (1985).
34. D. Cooke and M. J. Gidley, *Carbohydr. Res.* **227**, 103 (1992).
35. B. J. Goodfellow and R. H. Wilson, *Biopolymers* **30**, 1183 (1990).
36. S. G. Ring, P. Colonna, K. J. I'Anson, M. T. Kalichevsky, M. J. Miles, V. J. Morris and P. D. Orford, *Carbohydr. Res.* **162**, 277 (1987).
37. C. M. Durrani and A. M. Donald, *Polym. Gels Networks* **3**, 1 (1995).
38. R. E. Cameron, C. M. Durrani and A. M. Donald *Stärke* **46**, 285 (1994).
39. M. L. German, A. L. Blumenfeld, Ya. V. Guenin, V. P. Yuryev and V. B. Tolstoguzov, *Carbohydr. Polym.* **18**, 27 (1992).
40. M. Tako and S. Hizukuri, *J. Carbohydr. Chem.* **14**, 613 (1995).